Proceedings of 20th International Congress on Acoustics, ICA 2010

23–27 August 2010, Sydney, Australia

The use of acoustic actuation methods for microparticle manipulation within a droplet

Priscilla Rogers, Leslie Yeo and James Friend

Micro/Nanophysics Research Laboratory, Monash University, Clayton, Vic 3800, Australia

PACS: 43.25.Nm, 43.25.Qp

ABSTRACT

In this study, a high frequency (MHz–order) surface acoustic wave (SAW) device was used to simultaneously concentrate and separate two different sized particle types from the other within a microlitre droplet. This technique exploited two acoustic phenomena: drag force arising from acoustic streaming and acoustic radiation force. For a given particle size, it is possible to cause one phenomenon to dominate over the other. Exploiting these dependencies, 6 and 31 μm polystyrene particles were spatially separated and concentrated in a water droplet using a 20 MHz device within three seconds. This study shows widespread promise for the development of novel lab-on-a-chip devices for microparticle and cell manipulation based on acoustic actuation methods.

INTRODUCTION

Lab-on-a-chip (LOC) devices, which seek to conduct multiple analytical processes in parallel, offer numerous advantages over macroscale instruments, including decreased sample consumption, shortened reaction times, lower costs and increased portability (Whitesides 2006). Such microfluidic systems will have a large impact on numerous industries, including the defence, biomedical and pharmaceutical industries. The ability to manipulate microparticles and cells plays a key role in the success of LOC devices as the analyte of interest usually coexists in low concentrations amongst a myriad of other consituents within the fluid sample. Consequently, much research attention has been directed towards separating and/or isolating the analyte of interest from the other constituents within the sample.

The use of acoustically driven mechanisms for particle and cell manipulation are particularly advantageous as these techniques generally exhibit high throughput, have negligible physiological effects on cells, do not require tagging or moving parts, and are highly portable (Tsutsui and Ho 2009). Miniaturized surface acoustic wave (SAW) devices, in which an acoustic wave of nanometer–order amplitude propagates along the free surface of the substrate, have proven extremely suitable for LOC applications (Yeo and Friend 2009). For a fluid placed upon the substrate (Fig. (1)), strong absorption of incident SAW radiation occurs, whereby a longitudinal sound wave propagates into the droplet at the Rayleigh angle, θ_R, (Wixforth 2003) generating fast acoustic streaming. A suspended particle subject to this secondary streaming experiences a steady drag force. For microfluidic devices, in which the Reynolds number is typically of order one or less, the appropriate drag force on a spherical particle of radius R due to fluid flow is known as Stokes drag (F_D), which is defined by

$$F_D = 6\pi\mu UR, \tag{1}$$

where U and μ are the streaming velocity and the dynamic viscosity of the fluid, respectively. Furthermore, for a droplet subject to asymmetric SAW distribution, the three dimensional flow field is strikingly similar to Batchelor flows (Batchelor 1951), which cause the particles to convect along streamlines under the influence of drag to the lower portion of the droplet

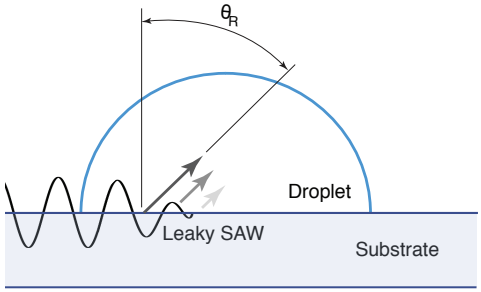

Figure 1: The SAW radiation is leaked into the droplet at the Rayleigh angle (θ_R) due to the mismatch in sound velocities, driving fast acoustic streaming within the droplet.

via a helical trajectory, where they concentrate at the stagnation point in the centre of the droplet (Raghavan et al. 2009).

The acoustic radiation force (i.e. net force attributed to the radiation pressure acting upon a particle's surface) can also be exploited for particle manipulation depending upon the sound field frequency (f) and particle size (R). Recently, SAWs were employed to generate a standing wave within a microfluidic channel for particle alignment and continuous particle separation (Shi et al. 2008; 2009). The radiation force acting on a suspended solid particle in an ideal fluid was first derived by King (King 1934). For a plane progressive wave, the radiation force ($F_{AR,L}$) is defined as

$$F_{AR,L} = 2\pi\rho\left(\frac{2\pi f}{c}\right)^4 R^6 |\dot{\xi}|^2 \frac{1+\frac{2}{9}\left(1-\frac{\rho}{\rho_p}\right)^2}{\left(2+\frac{\rho}{\rho_p}\right)^2} \tag{2}$$

for $\kappa R \ll 1$.

Here, ρ is the fluid density, $|\dot{\xi}|$ is the fluid particle velocity, c is the sound speed of the fluid medium, ρ_p is the particle density, and κ is the wave number. For larger particles (short

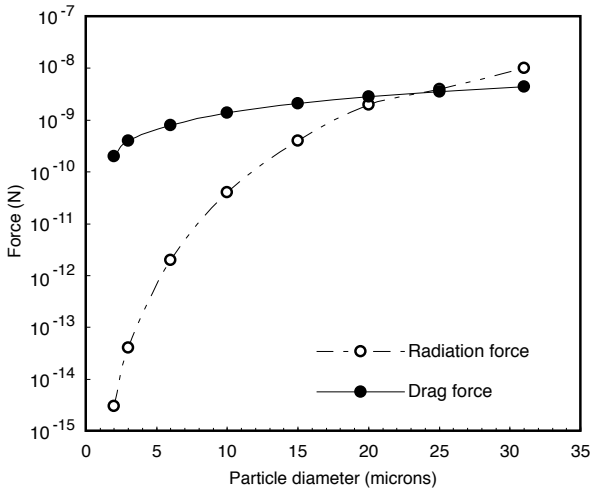

Figure 2: For a given sound field frequency, the radiation force increases rapidly with increasing particle size, scaling with R^6. The critical size range, defined as the range in which the order of magnitude of the two forces are equal, exists for particle sizes of 20—25 μm. Above this size range, the radiation force begins to dominate the drag force imposed by fluid streaming.

wavelength limit), $\kappa R \geq 1$, the higher power terms, $O(\kappa R)^8$ and higher, must be included (King 1934).

The goal of this research is to uniquely combine the acoustic radiation force and the drag force imposed by the fluid streaming to drive simultaneous particle concentration and spatial separation within a finite volume using a SAW device. Our primary interest in these acoustic forces is to make assessments of the conditions and design criteria required for one force to dominate over the other for a given particle size. A theoretical estimate of these forces reveals the ability to exploit each phenomenon using particle size as the only variable. These predictions are subsequently verified through experimental observations, following which particle separation and concentration based on particle size is demonstrated.

THEORETICAL ANALYSIS

In light of the goal of this research, it was necessary to theoretically estimate the magnitude of the acoustically induced forces acting upon a suspension of particles in a liquid droplet. Using Eqn. (1) and Eqn. (2) with higher order terms for larger particle sizes, it was possible to ascertain the relative contribution of each force on polystyrene particles (ρ_p = 1050 kg/m^3) with diameters ranging from 2 to 31 μm suspended in water (c = 1480 m/s, ρ = 1000 kg/m3) and placed on a 20 MHz SAW device (see Experiments). The fluid particle velocity amplitude, $|\xi|$, was assumed to be of the same order of magnitude as the SAW velocity amplitude on the piezoelectric substrate, which was experimentally measured using a laser Doppler vibrometer (MSA-400, Polytec Inc., Germany) as approximately 0.3 m/s. Average fluid streaming velocities, U, within the power range necessary to drive particle concentration (150– 600 mW) were estimated within microlitre droplet volumes (1.5 μL) using commercially available 2D particle tracking software (Diatrack 3.01, Semasopht, Switzerland) to be 15 mm/s. The corresponding forces are given in Fig. (2).

Fig. (2) highlights the rapid increase in the radiation force with increasing particle size, readily attributed to the fact that the acoustic radiation force scales with R^6, as opposed to the drag force, which scales with R. Compared to the drag force, the

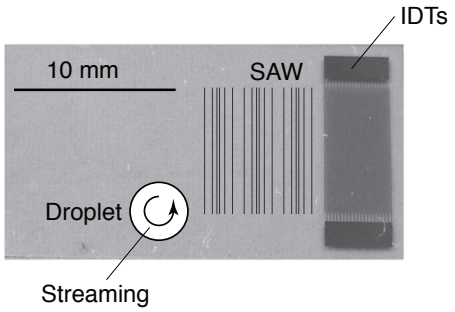

Figure 3: The SAW device consists of a piezoelectric substrate ($LiNbO_3$) and interdigital transducers (IDTs) to which power is supplied. The IDTs are fabricated via standard photolithography and wet etching techniques. The droplet is situated on the substrate such that approximately half of the droplet is subject to SAW radiation, as necessary for particle concentration in the centre of the droplet.

radiation force is considered negligible for smaller particle sizes, comparable for the 20 and 25 μm particle sizes, and greater for the 31 μm particle size. On this basis, it can be predicted that both acoustical phenomena will contribute to the largest particle size tested with the radiation force dominating particle behaviour, whereas the behaviour of the smaller particles will be purely dominated by the drag force imposed by acoustic streaming.

EXPERIMENTS

Device Description

The SAW device consisted of 0.5 mm thick, 128° rotated Y–cut, X–propagating lithium niobate substrate ($LiNbO_3$, Roditi, United Kingdom) as shown in Fig. (3). The dual layer (Aluminium/ Chromium) interdigital transducers (IDTs) comprised 20 straight finger pairs and were actuated at the characteristic resonant sinusoidal frequency f. The propagating SAW wavelength λ is defined by the IDT finger width and spacing, both of which are $\lambda/4$. Given a substrate sound velocity c_s of approximately 3980 m/s, and a finger width and spacing of 50 μm, the resonant frequency of the IDTs was approximately 20 MHz, as defined by $f = c_s/\lambda$.

Experiments

For all experiments, the input power was supplied to the SAW device by a signal generator (Rhode & Schwarz SML 01, Germany) and amplifier (Amplifier Research 10W1000C, USA). Both fluorescent (Thermo Scientific, Australia) and non-dyed (Bioscientific, Australia) polystyrene microspheres with diameters ranging from 2 to 31 μm were used. Each size was suspended individually in deionised water at concentrations on the order of 10^6 particles/mL. The 1.5 μL droplet was manually positioned off-centre such that approximately one half of its width was subjected to SAW radiation, as necessary for particle concentration (Li et al. 2007). The droplet was viewed using a stereomicroscope (Olympus BXFM, Japan) coupled with high speed videography (Olympus iSpeed, Japan for colour images and Mikotron, Germany for monochromatic images). Illumination was supplied by a mercury light source (EXFO X-Cite 120) and a proprietary 120 W short arc lamp (Olympus, Japan). For particle separation, 6 and 31 μm particles were suspended together maintaining their individual concentrations.

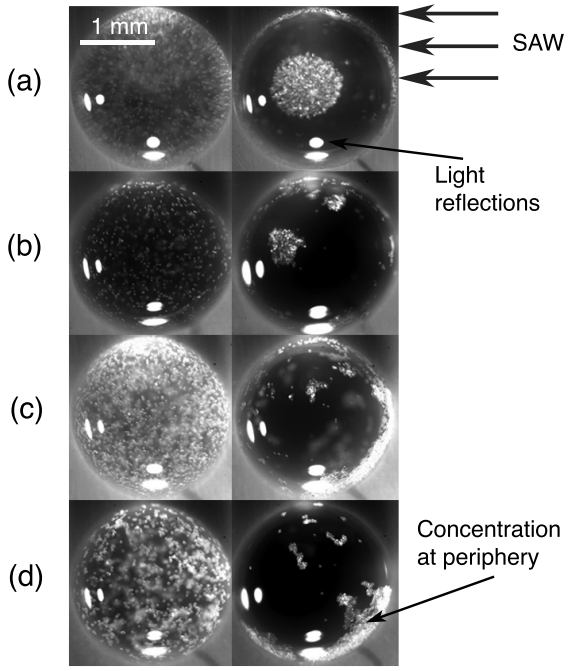

Figure 4: As theoretically estimated, the radiation force increases with increasing particle size. The radiation force is negligible for particle sizes of and smaller than (a) 15 μm particle sizes, and increasingly dominant for (b) 20 μm particle sizes, (c) 25 μm particle sizes, and (d) 31 μm particle sizes.

RESULTS AND DISCUSSION

For a given power, the change in particle behaviour for increasing particle sizes can be observed in Fig. (4). For particle sizes of 15 μm and below, the particles concentrate in the centre of the droplet under the influence of the drag force induced by acoustic streaming (Fig. (4a)) as previously studied (Li et al. 2007, Raghavan et al. 2009). Interestingly, for the 20 and 25 μm particles, Fig. (4b) and Fig. (4c) respectively, the particle concentration in the centre of the droplet becomes less evident as the particles are observed to be driven to the periphery of the droplet. This change in particle behaviour is in agreement with the theoretical analysis, which predicted that the radiation force and the drag force would contribute equally to particle behaviour within this size range: 20– 25 μm (defined as the critical size range). At the upper size limit, the 31 μm particles are observed to be almost entirely driven to the periphery (Fig. (4d)), except for a small sample that adhered to the substrate due to sedimentation prior to switching the power on. Aggregation at the periphery of the droplet can be explained by considering the directions of the acting forces. The radiation force acts in the direction of the Rayleigh angle (Fig. (1)) within the half of the droplet subject to SAW. Coupling this dominant force with a smaller drag force that forces the particles in a helical-like trajectory around the circumference of the droplet (Fig. 3), results in a net force that drives the particles to the periphery closest to the edge of the device (Rogers et al. 2010).

Based on these observations, the only prerequisite for separation at a given operating frequency is that one particle size is dominated by acoustic streaming (below the critical size range) and the other is dominated by the radiation force (above the critical size range). As such, 6 and 31 μm fluorescent particles were suspended in a single droplet. Figure (5) shows particle separation at an optimum input power of 420 mW as determined elsewhere (Rogers et al. 2010). The separation and concentration process is complete within just three seconds. For all powers tested, the 6 μm particles (green fluorescing) are observed to concentrate in the centre of the droplet almost immediately, with the concentration rate being dependent on the input power (Rogers et al. 2010). The 31 μm particles, on the other hand, are observed to be driven to the periphery of the droplet (Fig. (5), t = 0.2 s), as previously discussed.

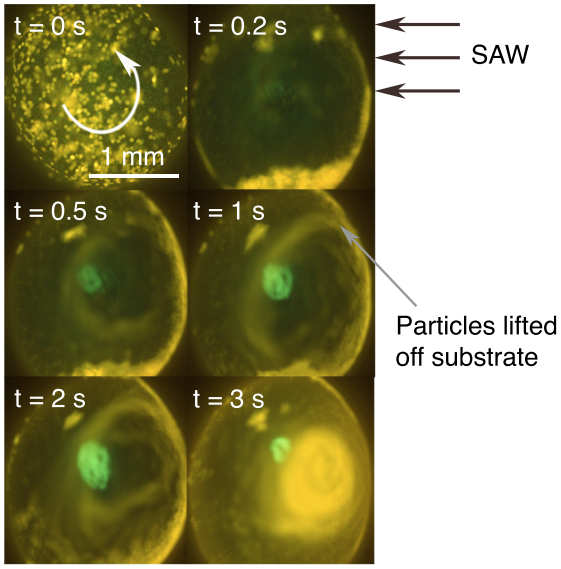

Figure 5: Separation of the 6 and 31 μm particles, green and yellow fluorescing respectively, at an input power of 420 mW. The 6 μm particles concentrate in the centre, within the bulk, of the droplet, whilst the 31 μm particles are driven to the periphery of the droplet followed by concentration on the free surface. The entire process is completed within three seconds.

In addition, a further interesting observation is made. Rather than the 31 μm particles remaining stationary at the periphery of the droplet as in Fig. (5) at t = 0.2 s, the smaller in magnitude drag force caused the particles to convect around the periphery of the droplet to the point of SAW radiation incidence as shown at t = 1 s. At this location, the particles were subsequently lifted off the substrate due to the dominant radiation force acting along the Rayleigh angle and subsequently concentrated on the free surface of the droplet (as opposed to the bulk). These findings indicate that another concentration mechanism is at play. The authors believe that shear-induced migration is in fact the underlying mechanism behind particle concentration on the free surface. During experimentation, it was noted that if the initial concentration of the 31 μm particles was below 10^6 particles/mL, concentration on the free surface became increasingly unlikely. This observation supports that shear–induced migration is the likely mechanism as this migration scheme is dependent upon an initial localised close packing fraction along the closed streamlines of the fluid flow being met before migration takes place to the low shear region (Leighton and Acrivos 1987), in this case located in the centre of the droplet.

The vertical spatial separation of the 6 and 31 μm particles present in Fig. (5) can be clearly seen by viewing the particles individually from the side. Figure (6) shows the 6 μm particles concentrating within the bulk towards the liquid-substrate interface, whilst the 31 μm particles concentrate on the free surface of the droplet. Furthermore, the 31 μm particles appear to concentrate about a slightly off-vertical polar axis at the top of the droplet (Fig. (5) and Fig. (6b)). This indicates that the acoustic streaming is not azimuthally centered around a vertical

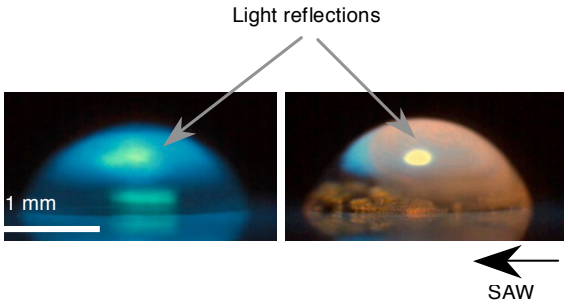

Figure 6: Images taken from the side of the droplet show the concentration of the 6 μm particles (left) within the bulk of the droplet, whilst the 31 μm particles (right) concentrate on the free surface.

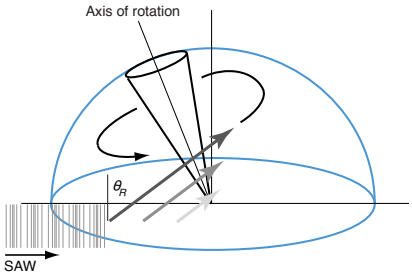

Figure 7: The azimuthal fluid flow component is in fact slightly skewed towards the IDTs. For visualisation purposes the SAW radiation is coming in from the left, as opposed to the right back corner in the prior images.

axis, rather it is centered around an axis slightly skewed towards the propagating SAW, which is due to the acoustic transmission into the droplet at the Rayleigh angle.

CONCLUSIONS

In this study, a high frequency SAW device was used to manipulate two particle types of different sizes suspended within a microlitre droplet. At MHz frequencies, two dominant forces, namely the radiation force and the drag force arising due to acoustic streaming, were observed to yield distinctively different particle behaviours. Generally, the drag force, which scales linearly with particle size, dominates for smaller particle sizes and drives the particles to concentrate within the centre of the droplet. As the particle size increases, however, the radiation force acting on the particle, which scales as the particle size to the sixth power, becomes increasingly comparable to the drag force, and dominates for particles larger than the critical size range. Consequently, the particles are driven to the periphery of the droplet, after which subsequent concentration on the free surface occurs. Accordingly, these forces were exploited successfully for the separation and concentration of 6 and 31 μm particles using a 20 MHz SAW device in just three seconds. These findings illustrate the possibility of using these two acoustic actuation methods for the ultrafast separation and concentration of cells and particles using microfluidic SAW devices.

REFERENCES

G. Batchelor. Note on a class of solution of the navier-stokes equations representing steady rotationally symmetric flow. *Q J Mech App Math*, 4:29–41, 1951.

L. King. On the acoustic radiation pressure of spheres. *Proc R Soc Lond Ser-A*, 147:212–240, 1934.

D. Leighton and A. Acrivos. The shear-induced migration of particles in concentrated suspensions. *J Fluid Mech*, 181: 415–439, 1987.

H. Li, J. Friend, and L. Yeo. Surface acoustic wave concentration of particle and bioparticle suspensions. *Biomed Microdevices*, 9:647–656, 2007.

R. Raghavan, J. Friend, and L. Yeo. Surface acoustic wave driven microcentrifugation. *Microfluid Nanofluid*, 8:73–84, 2009.

P. Rogers, J. Friend, and L. Yeo. Exploitation of surface acoustic waves to drive size dependent microparticle concentration within a droplet. *Lab Chip*, submitted, 2010.

J. Shi, X. Mao, D. Ahmed, A. Colletti, and T. Jun Huang. Focusing microparticles in a microfluidic channel with standing surface acoustic waves (SSAW). *Lab Chip*, 8:221–223, 2008.

J. Shi, H. Huang, Z. Stratton, Y. Huang, and T. Jun Huang. Continuous particle separation in a microfluidic channel via standing surface acoustic waves (SSAW). *Lab Chip*, 9: 3354–3359, 2009.

H Tsutsui and C Ho. Cell separation by non-inertial force fields in microfluidic systems. *Mech Res Commun*, 36:92–103, 2009.

G. Whitesides. The origins and the future of microfluidics. *Nature*, 442:368–373, 2006.

A. Wixforth. Acoustically driven planar microfluidics. *Superlattice Microst*, 33:389–396, 2003.

L. Yeo and J. Friend. Ultrafast microfluidics using surface acoustic waves. *Biomicrofluidics*, 3:012002, 2009.